



ISSN: 0067-2904
GIF: 0.851

New Approach for Determination of Oxonium Ion in Inorganic Acids by Quenched Fluorescence of Analytically Interested Species via the Liberated Bromine Using Continuous Flow Injection Laser Diode Fluorimeter Analyser

Issam M.A. Shakir, Raed F. Hassan*

Department of Chemistry, College of Science, University of Baghdad, Baghdad, Iraq

Abstract

A new method is characterized by simplicity, accuracy and speed for determination of Oxonium ion in ionisable inorganic acid such as hydrochloric (0.1 - 10), Sulphuric (0.1 - 6), nitric (0.1 - 10), perchloric (0.1 - 7), acetic (0.1 - 100) and phosphoric (0.1 - 30) (mMol.L^{-1}) acids. By continuous flow injection analysis. The proposed method was based on generation of bromine from the $\text{BrO}_3^- - \text{Br}^- - \text{H}_3\text{O}^+$. Bromine reacts with fluorescein to quench the fluorescence. A sample volume no.1 (31 μl) and no.2 (35 μl) were used with flow rate of 0.95 mL.min^{-1} using H_2O line no.1 as carrier stream and 1.3 mL.min^{-1} using fluorescein sodium salt line no.2. Linear regression of the concentration (mMol.L^{-1}) Vs quenched fluorescence gives a correlation coefficient of (89.33 - 99.72) for all studies of acids in various parameters were optimized. The proposed method was applied successfully for the determination of Oxonium ion in commercial samples. Using paired t-test between the newly developed method and classical method; shows that there were no significant differences between either methods. On this basis the new method can be accepted as an alternative analytical method for determination of Oxonium ion in commercial samples.

Keywords: Fluorescein sodium salt, Potassium bromide, Potassium bromated, Acids

طريقة جديدة لتقدير أيون الاوكسونيوم في الحوامض الاعضوية بواسطة تثبيط الفلورة لفصائل تحليلية مهمة من خلال توليد البروم الحر و باستخدام محلل الحقن الجرياني المستمر للفلورة بثنائيات وصلات ليزرية

عصام محمد علي شاكر، رائد فالح حسن*

قسم الكيمياء، كلية العلوم، جامعة بغداد، بغداد، العراق

الخلاصة

يعني البحث بمبدأ التداخل من خلال تفاعل ايون الاوكسونيوم مع مزيج من ايوني البروميد والبرومات كل يحقن في وصلة انموذج منفصلة من خلال صمامين منفصلين الاول (31 μl) والثاني (35 μl) وبمعدل جريان (0.95 mL.min^{-1}) للخط الاول كخط ناقل الماء و (1.3 mL.min^{-1}) للخط الثاني صبغة الفلورسين لتوليد البروم الحر (البرومين) الذي يتفاعل مع صبغة الفلورسين المتفلورة بأستخدام ليزر (405nm) لتثبيط الفلورة استخدمت الطريقة لتقدير الحوامض الاعضوية شائعة الاستعمال حيث أمكن تقدير (0.1 - 10) (ملي مول حامض الهيدروكلوريك، (0.1 - 6) (ملي مول حامض الكبريتيك، (0.1 - 10) (ملي مول حامض النتريك، (0.1 - 7) (ملي مول حامض البركلورك، (0.1 - 100) (ملي مول حامض الخليك و

*Email: Raed_alfoadi @ yahoo.com

(0.1 - 30) ملي مول حامض الفسفوريك . طبقت الطريقة بنجاح لتقدير ايون الاوكسونيوم في النماذج التجارية. باستخدام اختبار t-المزدوج لوحظ انه لا يوجد فرق جوهري بين الطريقتين المقترحة و القياسية ، وعلى هذا الاساس بالامكان استخدام الطريقة المقترحة للتحليل بالحقن الجرياني كبديل للطريقة القياسية.

Introduction

There are three common definitions for acids: Arrhenius definition, acids as substances which increase the concentration of hydrogen ions (H^+), or more accurately, oxonium ion (H_3O^+), when dissolved in water. Brønsted definition is an expansion: an acid is a substance which can act as a proton donor. By this definition, any compound which can easily be deprotonated can be considered an acid. Examples include alcohols and amines which contain O-H or N-H fragments. Lewis definition is a substance that can accept a pair of electrons to form a covalent bond. Examples of Lewis acids include all metal cations, and electron-deficient molecules such as boron trifluoride and aluminium trichloride [1]. Acids play important roles in the human body. Hydrochloric acid present in the stomach this aids in digestion by breaking down large and complex food molecules [2]. Many methods are available for determination of Oxonium ion but very limited work reported in the literature concerning Oxonium ion determination using fluorescence. A work based on the bromine released via $BrO_3^- - Br^- - H_3O^+$ reaction was used to decompose hydrogen peroxide and to release oxygen for the oxidation of lominul (5-amino phthyl hydrazide) with formation chemiluminescence light [3]. Spectrophotometric was used to determine acids via the release of bromine through $BrO_3^- - Br^- - H_3O^+$ [4], penetration of two reactant (mainly H_3O^+ and bromide ion) each injected in a separate loop but a delayed reaction coil and mixing to complete reaction. A carrier stream is bromated ion [5] and release of iodine from $IO_3^- - I^- - H_3O^+$ reaction [6]. Turbidimetric flow injection method was used in determination of hydrochloric acid by the reaction between potassium hexacyano ferrate(III) and copper (II) ion that eluted from cation exchange column by Oxonium ion to form dark green precipitate from complex $Cu_3[Fe(CN)_6]_2$ [7]. Chemiluminescence flow injection method play an important role in the determination of acids [8, 9] it was used to determination of Oxonium ion in strong acids by use strong ion exchange resin to adsorb-absorb cobalt (II) ion on resin bed, and displace cobalt(II) ion by Oxonium ion to decompose hydrogen peroxide and to release oxygen for the oxidation of lominul (5-amino phthyl hydrazide) with formation chemiluminescence light [10]. In this paper the bromine releases through $BrO_3^- - Br^- - H_3O^+$ reaction to quenched fluorescence for determination of acids.

Experimental

Chemicals

Stock solution of KBr(1M) was prepared by dissolving 119.0 g KBr per 1 liter, (0.3M) $KBrO_3$ was prepared by dissolving 50.106 g KBr per 1 liter and fluorescein sodium salt (uranine) ($C_{20}H_{10}Na_2O_5$) (0.01M) was prepared by dissolving 3.7627 g in 1 liter of distilled water. Different mineral acids (HCl , H_2SO_4 , HNO_3 , $HClO_4$, CH_3COOH , H_3PO_4) all were standardised against standard NaOH solution.

Apparatus and manifold

A homemade instrument linear array fluorometer-CFI analyser using laser (405 nm) as a source. Two channels of variable speed peristaltic pump (Ismatec type ISM 796), A rotary 6-port injection valve (Rheodyne, U.S.A) with a sample loop (0.5 mm id, Teflon, Variable length) used for sample injection. The output signals was recorded by x-t potentiometric recorder (KOMPENSO GRAPH C-1032) Siemens (Germany). Peak height was measured for each signal. Figure-1 shows the flow gram that was used for the determination and detection of Oxonium ion.

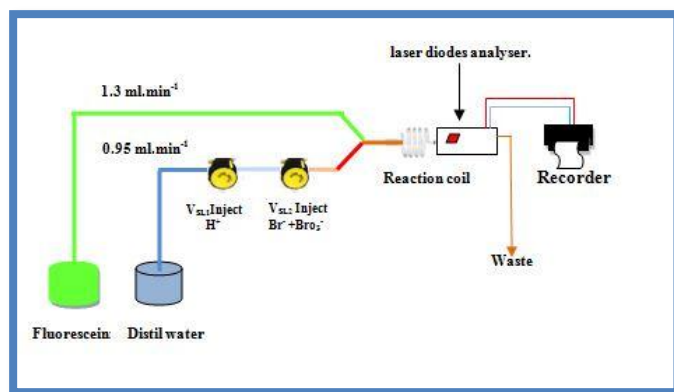


Figure 1- A schematic diagram of flow injection analysis system for determination of fluorescence using laser diodes CFIA analyser.

Methodology:

The flow diagram shown in Figure-1 is used for determination of oxonium ion in acids by the reaction between fluorescein sodium salt and generation of bromine by reaction $\text{BrO}_3^- - \text{Br}^- - \text{H}_3\text{O}^+$ to quenched fluorescence which is composed of two line: the first line is carrier stream (distilled water) at $0.95 \text{ mL}\cdot\text{min}^{-1}$ flow rate passes injection to carry oxonium ion sample volum no.1 ($31 \mu\text{l}$) and carry mixture ($(0.8 \text{ mMol}\cdot\text{L}^{-1})$ KBr and $(0.2 \text{ mMol}\cdot\text{L}^{-1})$ KBrO_3 . This will ensure that enough supply of Br^- and BrO_3^- ion) sample volum no.2 ($35 \mu\text{l}$), While the second line is the reagent supplies fluorescein sodium salt solution ($7 \text{ mMol}\cdot\text{L}^{-1}$) at $1.3 \text{ mL}\cdot\text{min}^{-1}$. Both lines meet at a junction (Y-junction), with an outlet for reactants product to pass through Homemade instrument Linear Array Fluormeter-CFI analyser. The responses were recorded on x-t potentiometric recorder to measure the quenched fluorescence.

Chemical Variables

Fluorescein sodium salt Concentration

New style of follow-up to choose the best conditions for the use of variables, which may be chemical or physical; obtained through responses as an example in this study is supposed to know the optimal concentration of a substance used in many fluorescein estimates during this project.

The followed method:

Solutions are prepared in different concentrations and the reasonable borders in sequence that acceptable by automatic array, for example in this study ($0.0-10 \text{ mMol}\cdot\text{L}^{-1}$) was chosen from fluorescein concentrations ($0.01, 0.05, 0.1, 0.5, 1, 5, 10$) $\text{mMol}\cdot\text{L}^{-1}$.

1. The responses were recorded in triplicate for each concentration. The results obtained are tabulated in Table-1

Table 1- Effect of fluorescein sodium salt ($\text{C}_{20}\text{H}_{10}\text{Na}_2\text{O}_5$) concentration on the measurement of energy transducer response.

$(\text{C}_{20}\text{H}_{10}\text{Na}_2\text{O}_5) \text{ mMol}\cdot\text{L}^{-1}$	Energy transducer response expressed as an average peak heights ($n=3$) \bar{y}_i in (mV)	RSD%	Confidence interval at (95%) $\bar{y} \pm t_{0.05/2, n-1} \sigma_{n-1} / \sqrt{n}$
0.01	0	0	0
0.05	4	0	4 ± 0
0.1	8	0	8 ± 0
0.5	189.333	4.88	189.333 ± 22.96
1	448	1.79	448 ± 19.88
5	1581.333	5.41	1581.333 ± 212.51
10	2166.667	0.53	2166.66 ± 28.70

2. Draw responses in the form of a curve between the responses obtained with a concentration wherein the response obtained is a function of the concentration. Shown in Figure-2.

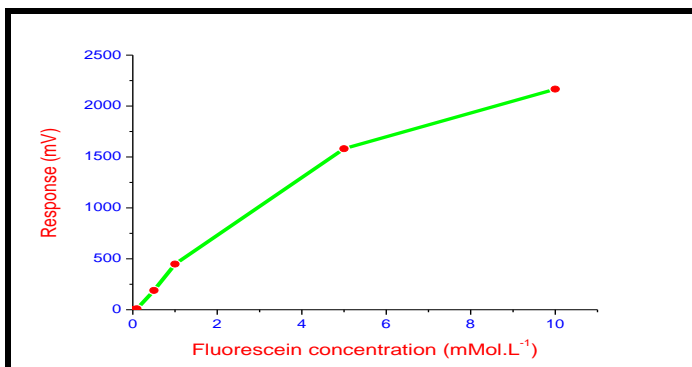


Figure 2- Variation of the fluorescein concentration, VS. variation for response.

3. The curve is divided into parts. The basis was the selection of concentration limits changes response was as follows division.
 - A. The first three points.
 - B. The first four points.
 - C. Curved area of the (1-5) mMol.L⁻¹.
 - D. Curved area of the (5-10) mMol.L⁻¹.
 - E. Curved area of all the points' linear function.
 - F. Curved area of all the points' parabola.

Followed by searching for a mathematical equation representing the data at the selected region. Possibly straight line equations from the class of $(y=a + bx)$. The best conditions to choose from is low slope (b) value and higher intercept (a) value. Table-2 shows the details line intercept of all the sections used. note that last column represents what is equivalent a parabola equation. While figure (2) is a planning document for each points to the Table-1, which shows the concentrations used and the responses obtained and the confidence interval (95%). Since the best section is the section between (5-10)mMol.L⁻¹. Selected (7mMol.L⁻¹) the best concentration that could be adapted to the priority area that were selected. As shown in Table-3 and Figure-3. This concentration will use of the subsequent studies.

Table 2- Selected linear segment properties (i.e.; slope and intercept) for optimization segment concentration.

	1 st three	1 st four	From(1-5) mMol.L ⁻¹	From(5-10) mMol.L ⁻¹	All point	Linear quadratic
a	-3.55	-1.67	1.65	9.96	8.82	-8.77
b	8.39	4.06	2.83	1.17	2.27	4.25

Table 3- Effect of fluorescein sodium salt(C₂₀H₁₀Na₂O₅) concentration on the measurement of energy transducer response.

(C ₂₀ H ₁₀ Na ₂ O ₅) .mMol.L ⁻¹	Energy transducer response expressed as an average peak heights (n=3) \bar{y}_i in (mV)	RSD%	Confidence interval at (95%) $\bar{y} \pm t_{0.05/2, n-1} \sigma_{n-1} / \sqrt{n}$
7	3560	0.97	3560±86.06

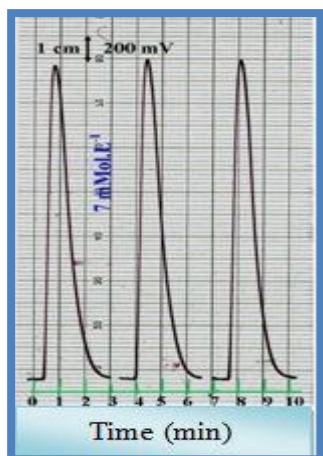


Figure 3-Variation of the transducer energy response (mV), VS. timeusing (7mMol.L⁻¹) fluorescein so dium salt.

Physical variables

Flow rate

Using optimum concentration of the reactant, fluorescein sodium salt (C₂₀H₁₀Na₂O₅) 7mMol.L⁻¹ & sample volume 18 μ l with a variable range 0.2 to 2.1 mL.min⁻¹ flow rate for the carrier stream for both of lines. The results obtained were summarized in Table-4. It was noticed at slow flow rate, there is an increase in dilution and dispersion which might cause an increase in base width Δt_B of response, while at flow rate (0.95 mL.min⁻¹) line no.1 and (1.3 mL.min⁻¹) for line no.2. very crucial concern was given for response peak heights and its sharpness Figure-4 and 5. The optimum flow rate used was based on the approximate similarities of the obtained energy transducer response i.e.; Calculating the standard deviation of all response obtained at variable flow rate indicate that percentage relative standard deviation (RSD% = 1.23) which can be regarded as there is no significant different of using any flow rate and can be regarded as the optimum flow rate .Therefore the selection of any flow rate will do as the optimum flow rate that can be used 0.95 & 1.3 mL.min⁻¹ for the first and second line successively were used.

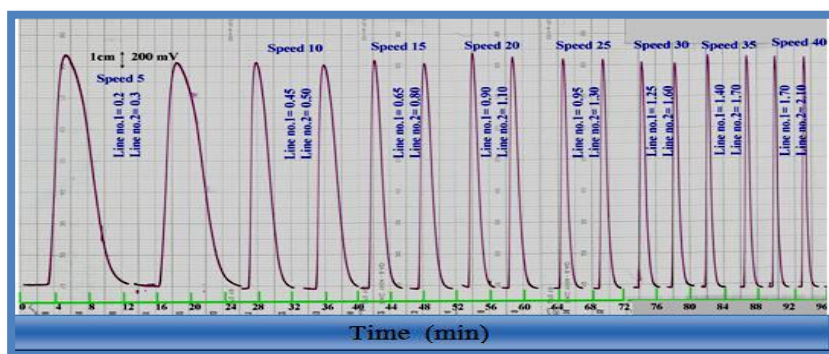


Figure 4- Effect of the variation of the flow rate on response profile.

Table 4- Flow rate effect on the measurement of energy transducer response.

Flow rate mL.min ⁻¹		Energy transducer response expressed as an average peak heights (n=3) \bar{y}_i in (mV)	RSD%	Confidence interval at(95%) $\bar{y} \pm t_{0.05/2, n-1} \sigma_{n-1} / \sqrt{n}$	Base width Δt_B (sec)
Line no.1	Line no.2				
0.2	0.3	3600	1.47	3600±131.47	444
0.45	0.5	3613.333	1.15	3613.333±103.44	228
0.65	0.8	3626.667	0.64	3626.667±57.36	144
0.9	1.1	3706.667	0.82	3706.667±75.91	108
0.95	1.3	3666.667	0.32	3666.667±28.70	84
1.25	1.6	3606.667	0.32	3606.667±28.70	72
1.4	1.7	3700	0.54	3700±49.70	66
1.7	2.1	3693.333	0.31	3693.333±28.70	60

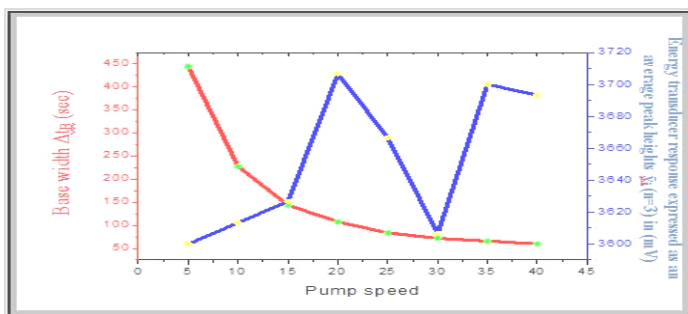


Figure 5- Effect of the variation of the flow rate on energy transducer response using (7mMol.L⁻¹) fluorescein. - Energy transducer response (mV), - Base width Δt_B

Sample volume

A- Use of valve no.1

The injected volume of sample was varied from 18 to 39 μL by changing the length of the sample loop in the injection valve, while the other chemical and physical parameters were remained fixed. An increase in the injection volume led to a significant increase in sensitivity and more fluorescence that can be shown in Table-5 and Figure-6, -7. Through tracking the Table-5 and diagram in Figure-7 which was divided into four segments (S), Designated as follows S_1 sample volume of (18-28) μL , S_2 sample volume of (28-31) μL , S_3 sample volume of (31-35) μL and S_4 sample volume of (35-39) μL . On the basis areas divided for sample volume by the new approach. Is a S_1 (18-28), S_2 (28-31), S_3 (31-35), S_4 (35-39) and S_5 (all points). The region of optimum sample volume is divided to five selected region or area of possible use followed by feuding the straight line equation for each sector area as shown in Table-6. Which tabulate the intercept and slope of each sector area. The lowest slope region is the puffered region (6.66) is the lowest possible obtained results which represent (28-31) μL . Also the intercept could be taken which should be the highest value; in order to have a platue region which changes in concentration should be at its lowest value. Therefore value of the sector 28 to 31 μL can be chosen to be the optimum sample volume range. 31 μL was chosen as the used volume for future work.

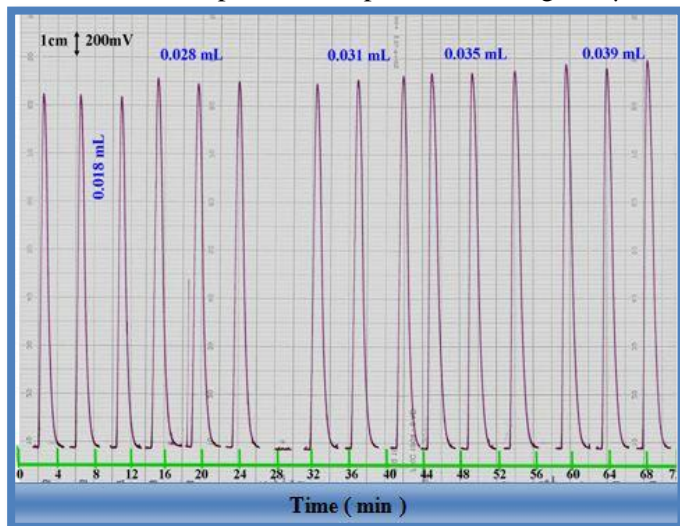


Figure 6- Effect of the variation of the sample volume in valve no.1 on response profile.

Table 5- Effect of the variation of sample volume in valve no.1 on the measurement of energy transducer response.

Sample volume μL	Energy transducer response expressed as an average peak heights (n=3) \bar{y}_i in (mV)	RSD%	Confidence interval at (95%) $\bar{y} \pm t_{0.05/2, n-1} \sigma_{n-1} / \sqrt{n}$	Base width Δt_B (sec)
18	3680	0.54	3680 ± 49.70	84
28	3820	1.05	3820 ± 99.36	96
31	3840	1.04	3840 ± 99.36	102
35	3926.667	0.29	3926.667 ± 28.70	102
39	4006.667	1.26	4006.667 ± 125.05	108

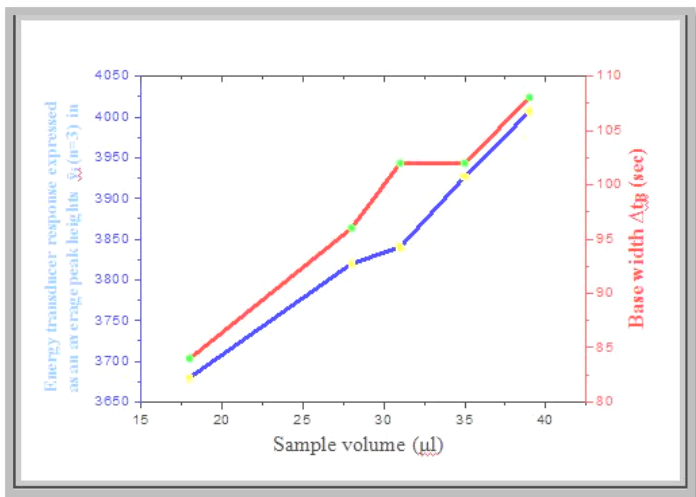


Figure 7- Effect of the variation of the sample volume in valve no.1 on energy transducer response using (7mMol.L⁻¹) fluorescein.

- energy transducer response (mV)
- Base width Δt_B

Table 6- Linear designed segment optimization for sample volume in valve no.1

	S ₁	S ₂	S ₃	S ₄	S ₅
a	3428.00	3633.33	3168.33	3226.67	3394.95
b	14.00	6.66	21.67	20.00	15.22

B- Use of valve no.2

The injected volume of sample was varied from 18 to 39 µL by changing the length of the sample loop in the injection valve, while the other chemical and physical parameters were remained fixed. An increase in the injection volume led to a significant increase in sensitivity and more fluorescence. Results of which are tabulated in Table-7 while Figure-8 shows kind of obtained responses. Figure-9 shows the plot of obtained responses Vs. sample volume.

Through tracking the Table-7 and diagram in Figure-9 which was divided into four segments (S), Designated as follows S₁ sample volume of (18-28) µl, S₂ sample volume of (28-31) µl, S₃ sample volume of (31-35) µl and S₄ sample volume of (35-39) µl. Dependable Stages of (18-39) µl is the best area for variable sample volume and then cancel the area 31 µl and replace the area S₂(28-35) and this will return to sample volume 31 µl; now if it is proved that area of segment (28-35) is the best area for sample volume on this basis areas divided for sample volumes by the new approach. Is a S₁(18-28), S₂ (28-35), S₃ (35-39) and S₄(all points). The region of optimum sample volume is divided to four selected region or area of possible use followed by finding the straight line equation for each sector area as shown in Table-8. Which tabulate the intercept and slope of each sector area. The lowest slope region is the preferred region (-6.67) is the lowest possible obtained results which represent (35-39) µl. Also the intercept could be taken which should be the highest value; in order to have a plateau region in which any changes in concentration should be at its lowest value. Therefore the value of the 35 to 39 µl sector can be chosen to be the optimum sample volume. 35µl was chosen as the used volume for future work.

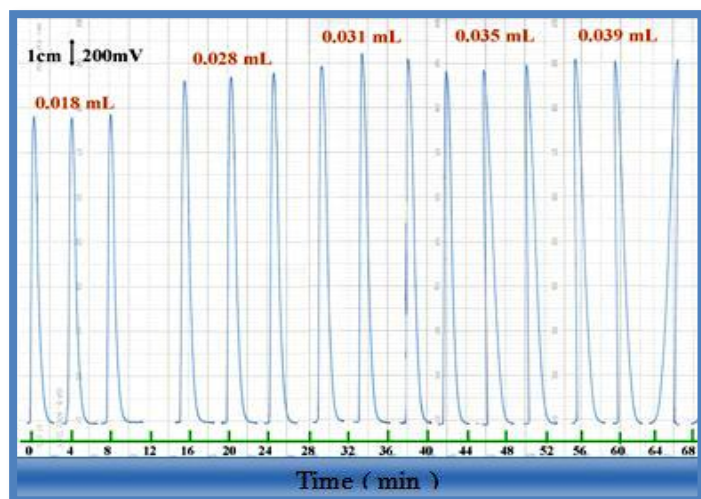


Figure 8- Effect of the variation of the sample volume in valve no.2 on response profile.

Table 7- Effect of the variation of sample volume in valve no.2 on the measurement of energy transducer response

Sample volume μl	Energy transducer response expressed as an average peak heights ($n=3$) \bar{y}_i in (mV)	RSD%	Confidence interval at (95%) $\bar{y} \pm t_{0.05/2, n-1} \sigma_{n-1} / \sqrt{n}$	Base width Δt_B (sec)
18	3446.667	0.34	3446.667 ± 28.70	72
28	3873.333	1.30	3873.333 ± 125.05	90
31	4080	1.77	4080 ± 179.13	84
35	4120	0.84	4120 ± 86.06	96
39	4093.333	0.28	4093.333 ± 28.70	84

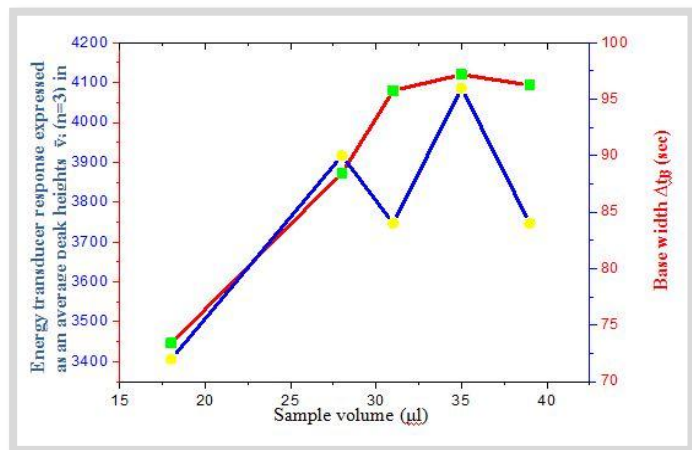


Figure 9- Effect of the variation of the sample volume in valve no.2 on energy transducer response using (7mMol.L⁻¹) fluorescein.

- Energy transducer response (mV)
- Base width Δt_B

Table 8- Linear designed segment optimization for sample volume in valve no.2

	S_1	S_2	S_3	S_4
a	2678.67	2886.67	4353.33	2916.32
b	42.67	35.24	-6.67	33.32

Purge time

A- Use of valve no.1.

The optimum sample segment of $31\mu\text{l}$ of 7 mMol.L^{-1} fluorescein was used and purged for a variable injection time periods ranging from 5 to 25 seconds. Also an open valve mode was used i:e leaving injection valve all the way through the end of measurements .Table-9 list all the obtained results while Figure-10 shows the kind of obtained profile response. While Figure-11 shows the response Vs. purge time.

Through tracking the table-9 and diagram in Figure-11 was divided into four segments (S), Designated as follows S_1 purge time (5-10)sec, S_2 purge time (10-15)sec, S_3 purge time (15-20)sec and S_4 purge time (20-25)sec . On the basis areas divided for purge time by the new approach. Is a S_1 (5-10), S_2 (10-15), S_3 (15-20) , S_4 (20-25) and S_5 (all points). The region of optimum purge time is divided to five selected region or area of possible use followed by finding the straight line equation for each sector area as shown in table (10) . The tabulated values of slope and intercept indicate that S_4 segment the best to choose. The obtained values shows that the region (20-25) sec is the best choice .So any point between (20-25) sec can be used as optimum. Therefore 25 sec was used.

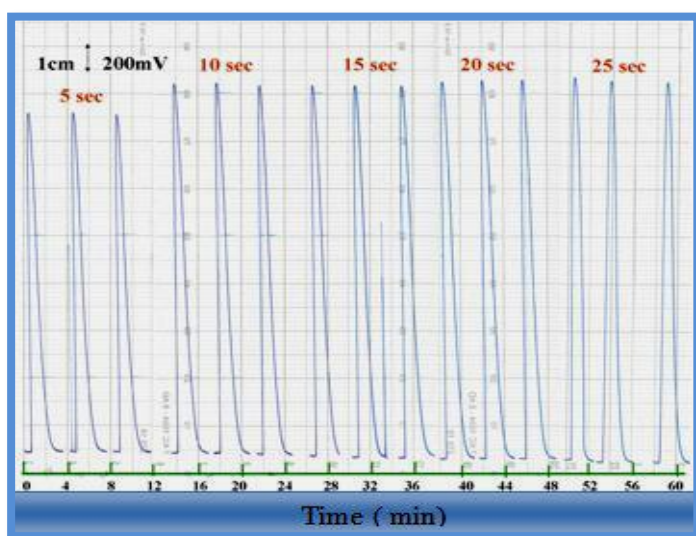


Figure 10- Effect of the variation of the purge time through valve no.1 on response profile.

Table 9- Effect of the variation of purge time through valve no.1 on the measurement of energy transducer response.

Purge time (Sec)	Energy transducer response expressed as an average peak heights (n=3) \bar{y}_i in (mV)	RSD%	Confidence interval at (95%) $\bar{y} \pm t_{0.05/2, n-1} \sigma_{n-1} / \sqrt{n}$
5	3593.333	0.32	3593.333 ± 28.70
10	3900	0.0	3900 ± 0.0
15	3940	0.0	3940 ± 0.0
20	4000	0.0	4000 ± 0.0
25	4033.333	0.29	4033.333 ± 28.70

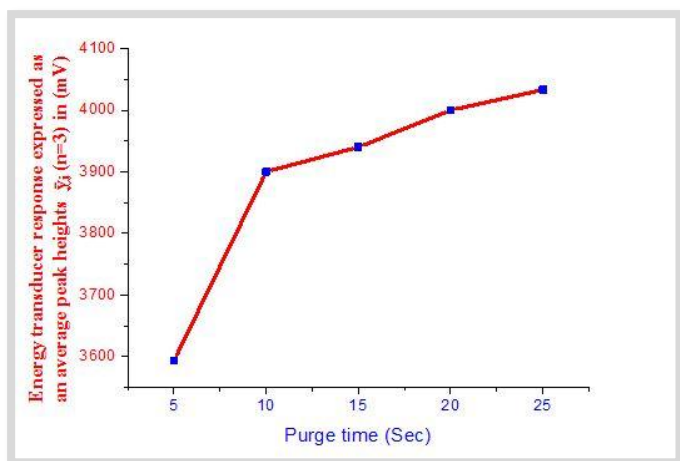


Figure 11- Effect of the variation of the purge time through valve no.1 on energy transducer response using (7mMol.L⁻¹) fluorescein.

Table 10- Linear designed segment optimization for purge time through volume in valve no.1

	S_1	S_2	S_3	S_4	S_5
a	3286.67	3820.00	3760.00	3866.68	3599.33
b	61.33	8.00	12.00	6.67	19.60

B- Use of valve no.2.

Variable purge times through valve no.2 ranging from 5 to 30 seconds were used. Also open valve mode was used. Table-11 tabulates all obtained values including confidence interval of each 3-successive measurement. While Figure-12 shows kind of obtained response profile. Figure-13 plots of the obtained responses Vs. purge time .It can be noticed that there are five segments (5-10) sec for S_1 while (10-15)sec for S_2 , (15-20) sec for S_3 ,(20-25) sec for S_4 and (25-30) sec for S_5 giving no. 1-6 for each individual point. It is quite difficult to allocate the optimum purge time as a single individual point therefore linear designed segment is used in choosing the optimum linear range based on the highest intercept value with lower slope value. It indicates from Table-12 that S_3 region is the most optimum region to choose from i: e; that (15-20) second, purge time is the optimum. Therefore any purge time starting from 15 till 20 seconds can be used. 20 seconds purge time was used through this work.

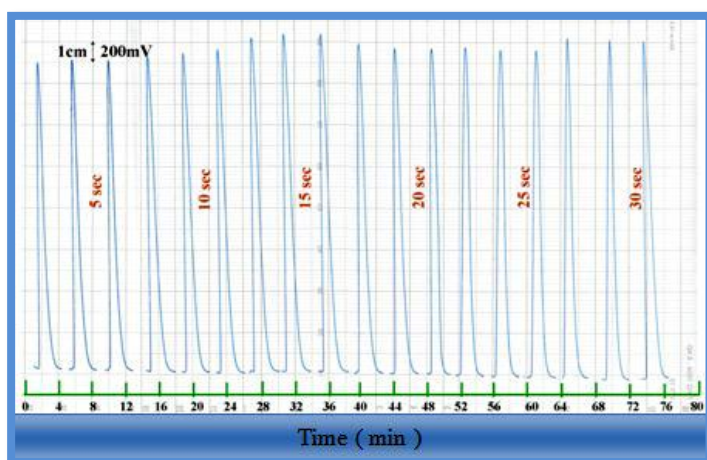
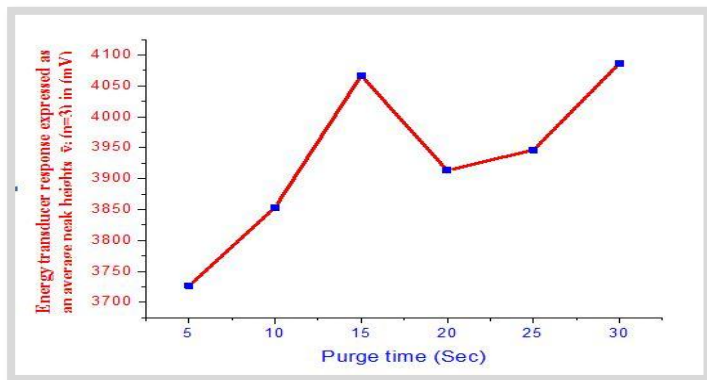


Figure 12- Effect of the variation of the purge time through valve no.2 on response profile

Table 11- Effect of the variation of purge time through valve no.2 on the measurement of energy transducer response.

Purge time (Sec)	Energy transducer response expressed as an average peak heights (n=3) \bar{y}_i in (mV)	RSD%	Confidence interval at (95%) $\bar{y} \pm t_{0.05/2, n-1} \sigma_{n-1} / \sqrt{n}$
5	3726.667	0.62	3726.667±57.36
10	3853.333	1.31	3853.333±125.05
15	4066.667	0.53	4066.667±53.66
20	3913.333	1.64	3913.333±159.73
25	3946.667	0.29	3946.667±28.70
30	4086.667	0.57	4086.667±57.36

**Figure 13-** Effect of the variation of the purge time through valve no.2 on energy transducer response using (7mMol.L⁻¹) fluorescein.**Table 12-** Linear designed segment optimization for purge time through volume in valve no.2

	S ₁	S ₂	S ₃	S ₄	S ₅
a	3600.00	3793.33	3780.00	3246.67	3739.56
b	25.33	6.00	6.67	28.00	11.01

Effect of coil length:

Variable coil length 0 – 100 cm was studied, this range of length comprises a volume of 0.00 – 0.785 ml which is connected before Y-junction directly in flow manifold system. Optimum concentration of fluorescein sodium salt (7mMol.L⁻¹), (3 mMol.L⁻¹) of HCl and Br⁻ ion as KBr (0.8 mMol.L⁻¹) and BrO₃⁻ as KBrO₃ (0.2 mMol.L⁻¹). With sample volume no.1 (31 μL) and sample volume no.2 (35 μL) were used. A study was carried out to the use of a delay reaction coil at position between V_{SL2} and the second reaction coil Figure-1. It was noticed that the use of no coil gave a better response profile. Figure-14 shows the detailed profile and Table-13 tabulate the obtained results of 0, 30, 60 and 100 cm length. The use of no coil gave most satisfactory result. Therefore no coil was used. While maintaining the second reaction coil.

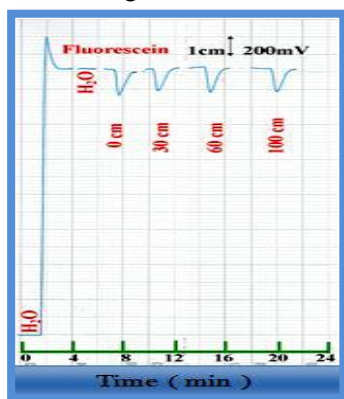
**Figure 14-** Effect of the variation coil length on response profile

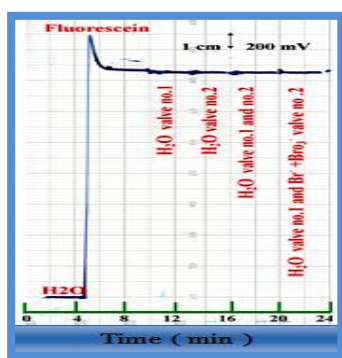
Table 13- Variation of coil length on energy transducer response.

Coil Length (cm)	Volume (ml) $r^2 \Pi h$ $r = 0.5\text{mm}$	Average transducer energy response expressed as peak heights (n=3) \bar{y}_i (mV)	RSD%	Confidence interval of The average response $\bar{y}_i \pm t_{0.05/2} \sigma_n - 1 / \sqrt{n}$
0	0.00	400	0	400±0.0
30	0.236	310	0	310±0.0
60	0.471	358.333	0	358.333±0.0
100	0.785	343.333	0.84	343.333±7.182

Effect of dilution on fluorescence:-

Through the use of manifold system described earlier Figure-15. Fluorescein sodium salt (7 mMol.L^{-1}) through the second line to maintain a constant fluorescence. Through the irradiation of (405 nm) laser diode. The introduction of distilled water to the system was studied as follows :-

It was noticed that in case of injection of distilled water through V_{SL1} ($31 \mu\text{l}$). While keeping V_{SL2} ($35 \mu\text{l}$) closed. No change in fluorescence was noticed. In case of closing V_{SL1} ($31 \mu\text{l}$) was injected of distilled water through V_{SL2} ($35 \mu\text{l}$). No signal change in fluorescence. Injection distilled water via V_{SL1} & V_{SL2} . No changes in fluorescence was noticed. This indicate that distilled water has no significant effect on fluorescence or the merging of fluorescein solution between the injected sample segment of king volume does not allow a variation to be noticed, which quite good that no noticeable difference can be captured by the detector and the speed of used flow rate. An additional experiment was carried out. Loading V_{SL1} with distilled water, while V_{SL2} was loaded with Br^- ion as KBr (0.8 mMol.L^{-1}) and BrO_3^- as KBrO_3 (0.2 mMol.L^{-1}). Proceeding in the measurement process leads to unchanged fluorescence response. It can be concluded that solute KBr and KBrO_3 has no effect on fluorescein. In the absence of acids.

**Figure 15-** Effect of dilution on the fluorescence**Calibration graph**

A series of different acids (HCl , H_2SO_4 , HNO_3 , HClO_4 , CH_3COOH and H_3PO_4) solutions ranging from (0.1 to 300) mMol.L^{-1} for each acid were prepared and injected at the established optimum condition. The results obtained and variation of oxonium ion concentration at $31 \mu\text{L}$ sample volume V_s quenched fluorescence response of linear array laser diode fluorimeter analyser as shown in Figure-16(A,B,C,D,E and F). While a scatter plot diagram was constructed between the variations of the quenched fluorescence responses versus concentration of acids showing a linear dynamic range extended from (0.1 to 300) mMol.L^{-1} Figure-17 (A, B, C,D,E and F). Table-14 tabulates correlation coefficient, linear percentage, straight line equation and the calculated t -value at 95% confidence; which is larger than tabulated t -value indicating clearly that the linearity against non-linearity is accepted to quenched response of linear array laser diode fluorimeter analyser, When using (0.8 mMol.L^{-1}) KBr and (0.2 mMol.L^{-1}) KBrO_3 . This will ensure that enough supply of Br^- and BrO_3^- ion are available as soon as through a required by extra acid that might be used through the research work.

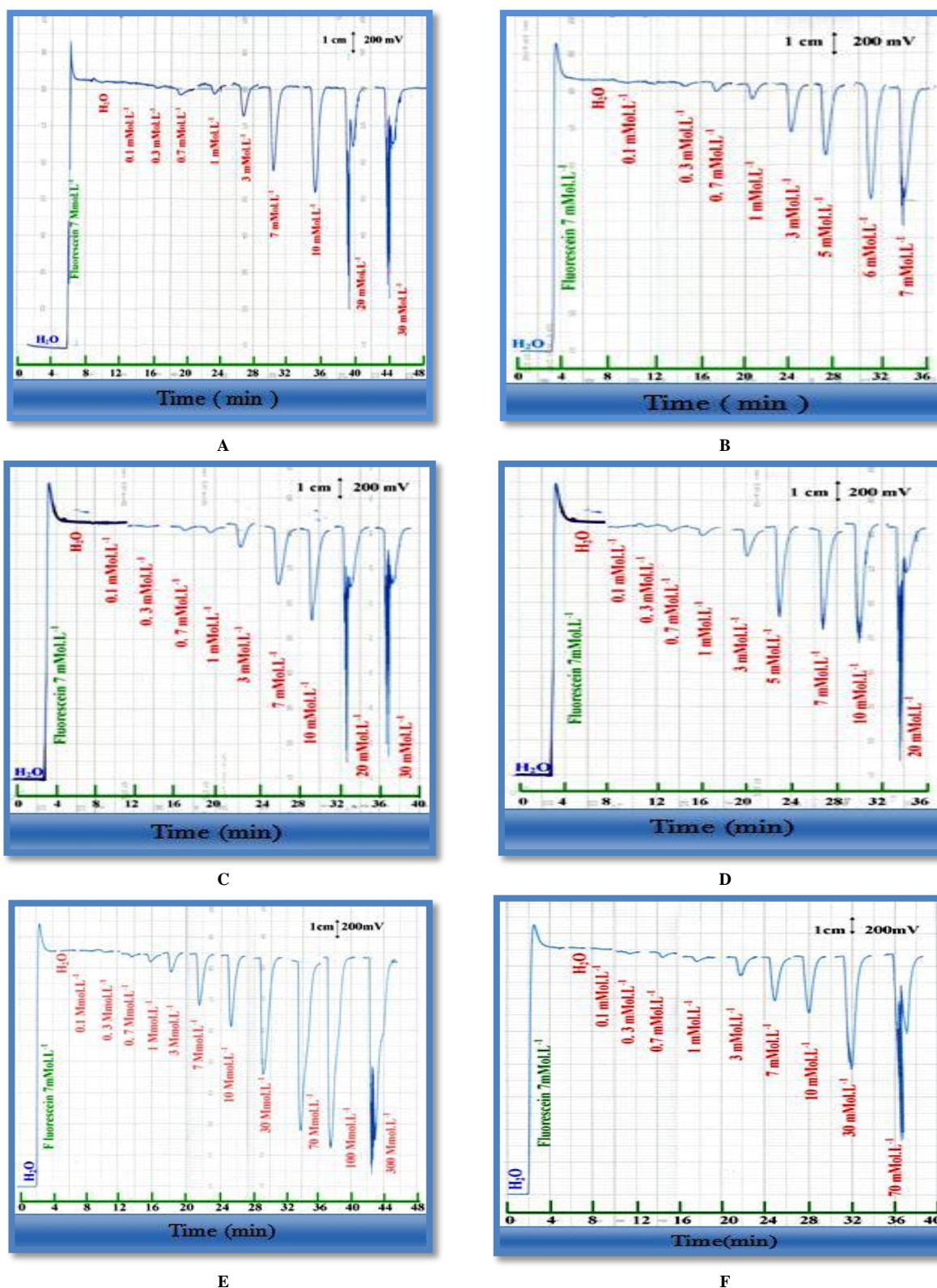


Figure 16- Effect of the variation of concentration on fluorescence response (A-HCl, B- H₂SO₄, C-HNO₃, D- HClO₄, E-CH₃COOH and F- H₃PO₄)

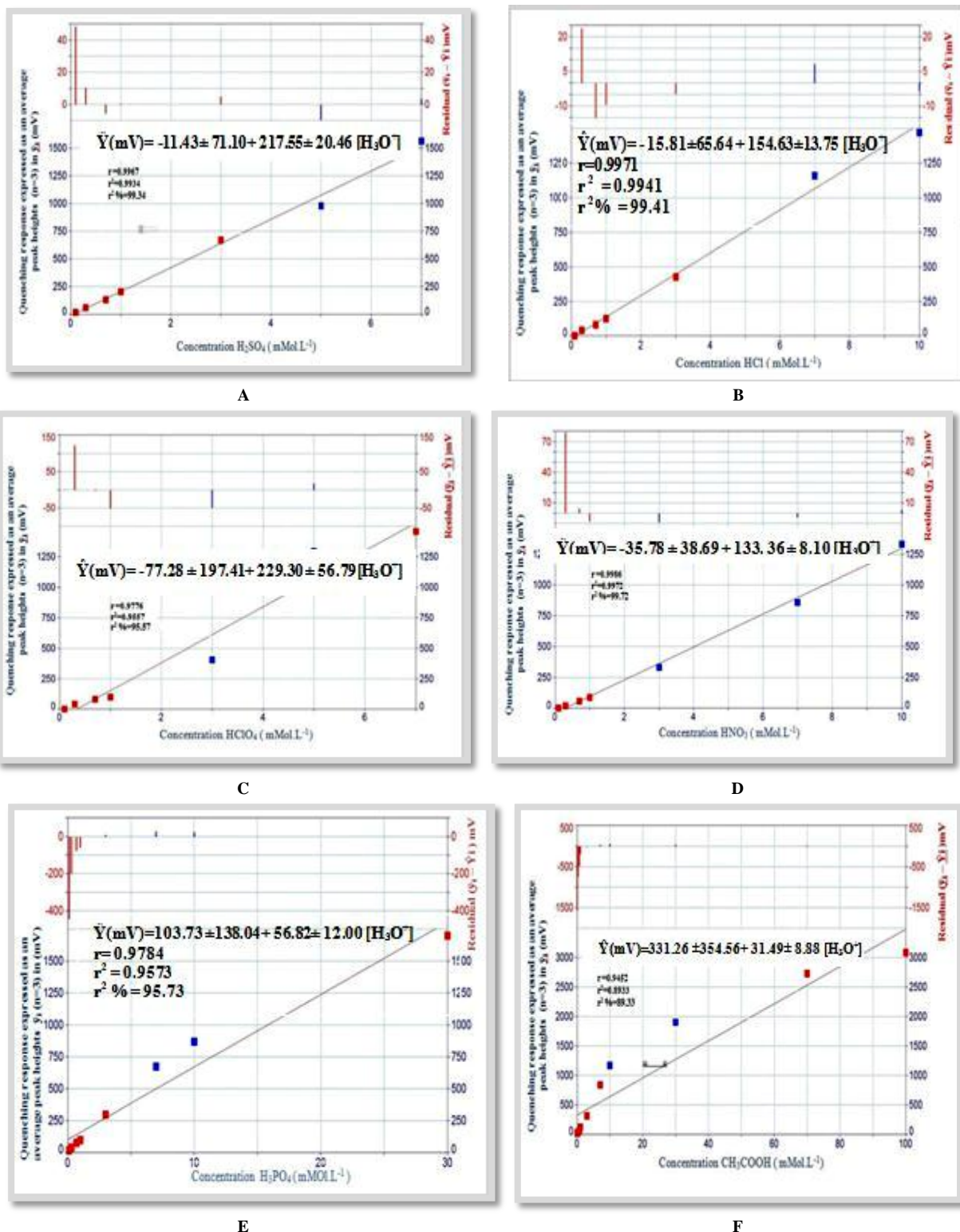


Figure 17- Calibration graph for the variation of concentration on: -
 A: Quenched fluorescence response expressed by linear equation using laser diode fluorimeter analyser,
 B: Residual ($\bar{y}_i - \hat{Y}_i$), \bar{y} : practical value, \hat{Y}_i : estimate value
 (A-HCl, B- H_2SO_4 , C- HNO_3 , D- $HClO_4$, E- CH_3COOH and F- H_3PO_4)

Table 14- Summary of linear regression for the variation of quenched fluorescence response with acids concentration using simple regression line of the form ($\hat{Y} = a+bx$) at optimum conditions.

Type of acid	Measured $[H_3O^+]$ mMol.L ⁻¹	Linear dynamic range $[H_3O^+]$ mMol.L ⁻¹	$\hat{y} = a \pm S_a t + b \pm S_b t [H_3O^+]$ mMol.L ⁻¹ at confidence interval at 95%, n-2	r r^2 r^2 %	table no. at 95%, n-2	Calculated $L_{value} = \frac{t/\sqrt{n-2}}{\sqrt{1-r^2}}$
HCl	0.1-30	0.1 - 10 n=7	$-15.81 \pm 65.64 + 154.63 \pm 13.75 [H_3O^+]$	0.9971 0.9941 99.41		2.571 << 28.918
H ₂ SO ₄	0.1-7	0.1- 6 n=7	$-11.43 \pm 71.10 + 217.55 \pm 20.46 [H_3O^+]$	0.9967 0.9934 99.34		2.571 << 27.345
HNO ₃	0.1-30	0.1-10 n=7	$-35.78 \pm 38.69 + 133.36 \pm 8.10 [H_3O^+]$	0.9986 0.9972 99.72		2.571 << 42.315
HClO ₄	0.1-20	0.1-7 n=7	$-77.28 \pm 197.41 + 229.30 \pm 56.79 [H_3O^+]$	0.9776 0.9557 95.57		2.571 << 10.381
CH ₃ COOH	0.1-300	0.1-100 n=10	$331.26 \pm 354.56 + 31.49 \pm 8.88 [H_3O^+]$	0.9452 0.8933 89.33		2.306 << 8.182
H ₃ PO ₄	0.1-70	0.1-30 n=8	$103.73 \pm 138.04 + 56.82 \pm 12.00 [H_3O^+]$	0.9784 0.9573 95.73		2.447 << 11.591

\hat{Y} (mV) = Estimated response measurement (n=3) for each single concentration, r =correlation coefficient, r^2 %: linearity percentage

Limit of Detection (L.O.D)

A study was carried out to determine the limit of detection of oxonium ion via successive gradual dilution of the minimum concentration in the linear range. Table-15 shows the limit of detection conducted by linear range equation and corrected limit of detection (L.O.D) based on dilution factor (D.F).

Table 15- Limit of detection of oxonium ion at optimum parameters for each acid

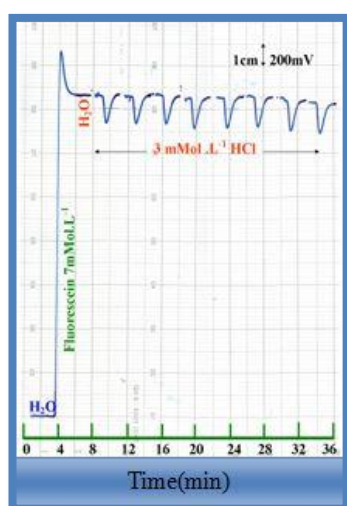
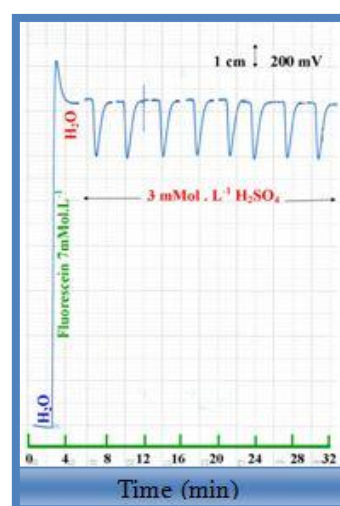
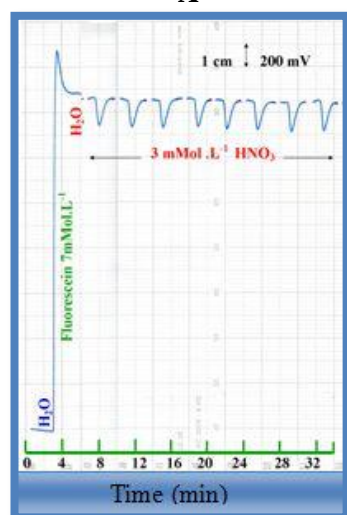
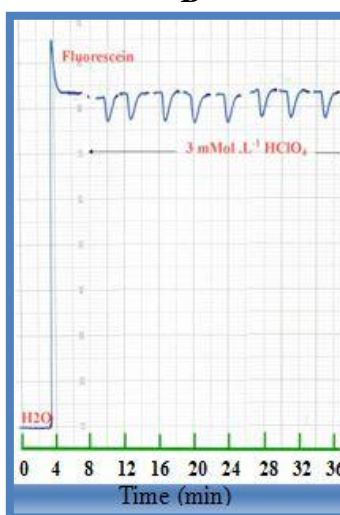
Type of acid	Practically based on the gradual dilution for the minimum concentration	Corrected limit of detection(L.O.D)based on dilution factor(D.F)
HCl	113 ng/sample	0.79 ng/sample
H ₂ SO ₄	304 ng/sample	2.13 ng/sample
HNO ₃	195 ng/sample	1.37 ng/sample
HClO ₄	311 ng/sample	2.18ng/sample
CH ₃ COOH	186 ng/sample	130 ng/sample
H ₃ PO ₄	303 ng/sample	2.12 ng/sample

Repeatability

The repeatability of measurement and the efficiency of homemade linear array laser diode fluorimeter analyser were studied at fixed concentrations for one of the used acids ((HCl , H₂SO₄ , HNO₃ ,HClO₄) (3mMol.L⁻¹), CH₃COOH and H₃PO₄ (10mMol.L⁻¹)) using the optimum parameters. Repeated measurements for eight successive injections were measured the obtained results are tabulated in Table no.(16) which shows that the percentage relative standard deviation was indicate clearly the trust ability of the adopted methodology us linear array laser diode fluorimeter analyser. Figure-18(A, B, C, D, E and F) shows a kind of response-time profile for the used concentrations.

Table 16- Repeatability of successive measurements for acids at (31 μ L)

Type of acid	No. of measurement	Incident light response expressed as peak height (mV)	Average \bar{y}_i mV	RSD %	confidence interval of the mean $\bar{y} \pm t_{0.05/2, n-1} \sigma n^{-1} / \sqrt{n}$
HCl	8	350,350,360,360, 360,360, 360, 360	357.5	1.30	357.5 ± 3.871
H ₂ SO ₄	8	640,640,640,640, 640,640,640,640	640	0.0	640 ± 0.0
HNO ₃	8	320,,320,330,330, 330,330,330,330	327.5	1.41	327.5 ± 3.871
HClO ₄	8	310,310,310,310, 320,320,310, 310	312.5	1.48	312.5 ± 3.871
CH ₃ COOH	8	1160,1160,1160, 1160,1160,1140, 1160,1140	1155	0.80	1155 ± 7.743
H ₃ PO ₄	8	860, 860, 860, 860, 860, 860, 860, 860,	860	0	860 ± 0.0

**A****B****C****D****Figure 18-** A Profile of successive repeatability measurements of (A)HCl,(B) H₂SO₄, (C)HNO₃, and (D)HClO₄ using linear array laser diode fluorimeter analyser.

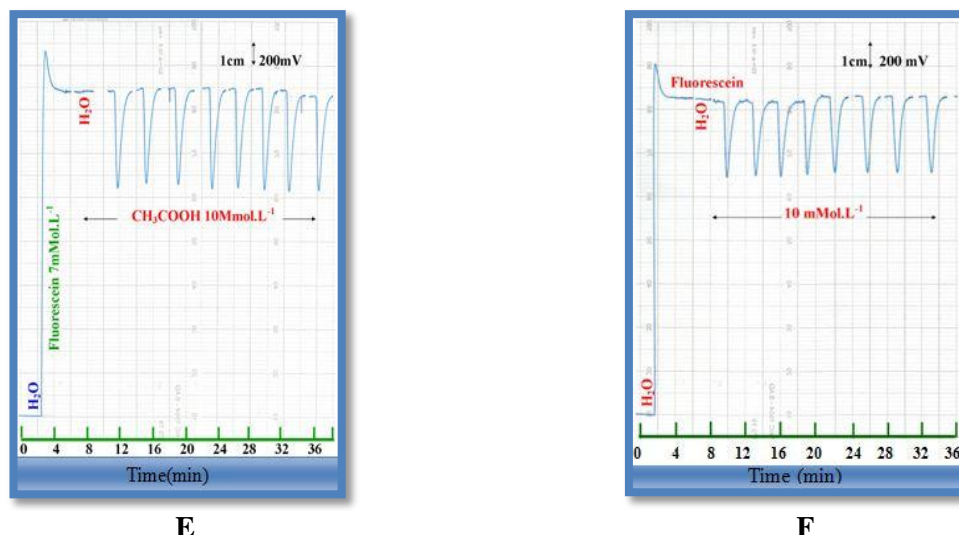


Figure 18- A Profile of successive repeatability measurements of (E) CH₃COOH and (F) H₃PO₄ using linear array laser diode fluorimeter analyser.

Selection of types and acid concentration:

Different acid of variable concentration were used as can be shown in Figures-16 and 17 (A,B,C,D, E and F) . All the results obtained are tabulated in Table-14 a summarized data of linear regression which is represented by slope and intercept. Sulphuric acid was the choice of (3-5 mMol.L⁻¹). Other acid e.g. (HCl , H₂SO₄ , HNO₃ , HClO₄, CH₃COOH and H₃PO₄) was not used due to the effect of thier oxidizing effect. Which might cause an interferences. While the effect of acetic acid and phosphoric acid was eliminated due to weak sensitivities represented by their slopes.

Calibration graph by Classical method:

Calibration graph of classical method (measurement of pH by HANNA Instrument, pH 211 Microprocessor pH Meter) for the determination of [H₃O⁺] in acids for the range of 0.001 to 1000mMol.L⁻¹. Table-17 tabulates all the obtained data for the classical method.

Table 17- Summary of linear regression for the variation of pH with acids concentration using simple regression line of the form ($\hat{Y} = a+bx$) at optimum conditions.

Type of acid	Measured [H ₃ O ⁺] mMol.L ⁻¹	Linear dynamic range [H ₃ O ⁺] mMol.L ⁻¹	$\hat{y} = a \pm S_a t + b \pm S_b t$ [H ₃ O ⁺] mMol.L ⁻¹ at confidence interval at 95%, n-2	r r^2 r^2 %	$t_{\text{table no. at 95\%, n-2}}$	Calculated $t_{\text{value}} = \frac{t/\sqrt{n-2}}{\sqrt{1-r^2}}$
HCl	0.001-1000	3-70 n=5	$166.85 \pm 19.25 + 0.81 \pm 0.56$ [H ₃ O ⁺]	0.9364 0.8768 87.68		3.182 << 4.621
H ₂ SO ₄	0.001-1000	5-70 n=6	$173.35 \pm 14.84 + 0.81 \pm 0.47$ [H ₃ O ⁺]	0.9227 0.8513 85.13		2.776 << 4.786
HNO ₃	0.001-1000	3-30 n=5	$156.23 \pm 16.53 + 1.500 \pm 0.97$ [H ₃ O ⁺]	0.9431 0.8894 88.94		3.182 << 4.913
HClO ₄	0.001-1000	7-100 n=6	$176.92 \pm 11.21 + 0.49 \pm 0.21$ [H ₃ O ⁺]	0.9540 0.9101 91.01		2.776 << 6.364
CH ₃ COOH	0.001-1000	7 - 100 n=5	$100.28 \pm 9.88 + 0.30 \pm 0.18$ [H ₃ O ⁺]	0.9542 0.9105 91.05		3.182 << 5.523
H ₃ PO ₄	0.001-1000	7 - 100 n=5	$152.98 \pm 10.77 + 0.34 \pm 0.19$ [H ₃ O ⁺]	0.9563 0.9145 91.45		3.182 << 5.666

\hat{Y} (mV) = Estimated response, r = correlation coefficient, r^2 %: linearity percentage

Application

Two methods were used for the determination of oxonium ion H_2SO_4 (98%, Loba Chemie, country: India), Apple vinegar and white vinegar in commercial samples. The methods were used first method was linear array laser diode fluorimeter analyser -Continuous flow injection analyser, While the second method was pH meter. A series of solution were prepared of H_2SO_4 sample by transferring 10 mL to each of the six volumetric flask (50 ml), followed by the addition of (0,1,2,3,4,5) mL from 20 mMol.L⁻¹ standard solution of H_2SO_4 in order to have the concentration range from (0-2) mMol.L⁻¹. Flask no.1 is the sample flask volume, A series of solution were prepared of Apple vinegar and white vinegar sample by transferring 5 mL to each of the six volumetric flask (50 ml), followed by the addition of (0,2,4,6,8,10) mL from 100 mMol.L⁻¹ standard solution of CH_3COOH in order to have the concentration range from (0-20) mMol.L⁻¹. Flask no.1 is the sample flask volume. Table-18 shows the summary of standard additions method results from the three samples with the amount of oxonium ion in acids samples. Using paired t-test between the newly developed method and classical method; as shown in Table-19 shows no significant differences between either method that can be described.

Table 18- Results for determination of oxonium ion in real sample by two methods using standard addition

Type of Sample	Equation of standard additions curve at 95%,n-2 $\hat{Y}_{(mV)}=a+ b [X]$ $\hat{Y}_{(FTU)}=a+ b [X]$	r r^2 $r^2\%$	oxonium ion mMol.L ⁻¹ In 50 mL Sample	t_{tab} at 95 % (n-2)	Calculated t-value $\frac{ r \sqrt{n-2}}{\sqrt{1-r^2}}$
laser diode fluorimeter analyser CFIA					
HANNA Instrument, pH 211 Microprocessor pH Meter					
H_2SO_4	983.78+237.64 [X]	0.9851 0.9705 97.05 %	20.70 mMol.L ⁻¹		2.776 << 11.46
	97.04+ 23.76 [X]	0.9925 0.9851 98.51 %	20.40 mMol.L ⁻¹		2.776 << 16.28
Apple vinegar	471.62+ 44.37 [x]	0.9832 0.9666 96.66%	106.3 mMol.L ⁻¹		2.776 << 10.77
	48.28 + 4.34 [x]	0.9960 0.9920 99.20%	111.2 mMol.L ⁻¹		2.776 << 22.31
white vinegar	725.19+ 65.96 [x]	0.9978 0.9956 99.56%	109.9 mMol.L ⁻¹		2.776 << 30.15
	56.78+ 5.04 [x]	0.9971 0.9943 99.43%	112.7 mMol.L ⁻¹		2.776 << 26.30

\hat{Y}_i = Estimated response (mV), [X]: Oxonium ion mMol.L⁻¹,

r= correlation coefficient, r^2 % = linearity percentage, n= no.of measurement for each methods =6.

Table 19- Summarize Paired t-test between new method and classical method (pH meter) using standard addition

Type of acid	Type of method	X	X d	$\bar{x}d$	σ_{n-1}	$t_{cal} = \frac{\bar{x}d\sqrt{n}}{\sigma_{n-1}}$
H_2SO_4	F. Method	4.14	0.06	0.28	0.22	4.303 >> 2.20
	PH. Method	4.08				
Apple vinegar	F. Method	10.63	0.49			
	PH. Method	11.12				
white vinegar	F. Method	10.99	0.28			
	PH. Method	11.27				

F. method: Response of linear array laser diode fluorimeter analyser CFI analyser (Concentration(mMol.L⁻¹)).

pH method: Reading of pH meter (Concentration (mMol.L⁻¹)).

$\bar{x}d$: Mean for difference(Concentration (mMol.L⁻¹)) between F. method and pH meter reading.

σ_{n-1} : Standard deviation .

n= 3 response measurement for each single concentration

tcal. : t calculated

Conclusion

The proposed method is simple, rapid, speed and sensitive for determination of Oxonium ion. The method based on reaction between generation bromine by Oxonium ion from the BrO_3^- - Br^- - H_3O^+ reaction. The new method can be used to determine of Oxonium ion in pure and commercial sample.

References

1. Ebbing, D.D. and Gammon. **2005**. *General chemistry*. 8th Edn. Boston, MA-Houghton Mifflin.
2. David L. N. and Michael M. C. **2000**. *Lehninger principles of biochemistry*. 4th Edn. The American Association for the Advancement of Science.
3. Shakir, I.M.A. and Faizullah, A.T.**1990**. Determination of Oxonium ion in strongly ionisable inorganic acids and determination of substituted acetic acid using flow injection and chemiluminescence detection. *Analyst*,115, pp:69-72.
4. Shakir, I.M.A.**1990**. New approach for the determination of inorganic acids, and selected derivatives of acetic acid by flow injection analysis. *J.Coll.Education, Salahadin University*, 2(3), pp:225-232.
5. Turky.N.S.**2000**. A noble semi- automated spectrophotometric determination of micro amounts of acids via zone penetration techniques. *Iraqi J.Sci*, 41A(2),pp:42-58.
6. KamSon, O. F. **1986**. Spectrophotometric Determination of Iodate and Acids. *Anal.Chim. Acta*, 179,pp:475-477.
7. Shakir, I.M.A. and Mansoor.A.A.**2014**. Novel method for determination of hydrochloric acid via ion exchange and precipitation reaction indirectly by using linear array ayah 5SX1-T-1D continuous flow injection analyser. *Research Article*. 4(4), pp: 763-776.
8. Kiba.N., Tachibana.M., Tani.K. and miwa.T.**1998**. *Anal.Chim.Acta*. 375(1-2), pp: 65-70.
9. wang.S.,Du.L.,wang.L. and Zhuang.H.**2004**. Determination of pipemidic acid based on flow-injection chemiluminescence due to energy transfer from peroxyntrous acid synthesized on-line *Anal.Sci*.20, pp: 315-317.
10. Shakir, I.M.A. and Hassan.R.F.**2009**. A novel method for the determination of Oxonium ion in strong acid via flow injection- chemiluminescence. Proceeding of 3rd scientific conference of the College of Science, University of Baghdad.pp:1637-1646.